Optimal Takeoff Trajectories of a Heavily Loaded Helicopter

FREDRIC H. SCHMITZ*
Department of the Army, Ames Research Center, Moffett Field, Calif.

Optimal control theory has been applied to the STOL takeoff of a heavily loaded helicopter. The object of the analysis was to determine constrained and unconstrained extremal trajectories that maximize the terminal vertical distance for a given fixed horizontal distance. The resulting optimal trajectory consists of an initial acceleration segment followed by a decelerating segment in which most of the terminal altitude is gained. If the problem was constrained to nondecelerating flight, the resulting optimum consisted of a maximum acceleration segment followed by a constant velocity climbout segment. The slightly decreased performance of the constrained optimum was more than offset by its ease of implementation.

Nomenclature

A = area of rotor disc
C_{1-5} = momentum theory expansion coefficients
CPL = power loss
cg = helicopter center of gravity
f = wetted drag area of HLD helicopter
f_0 = the derivative of the payoff function with respect to time
g = acceleration of gravity
HLD = heavily loaded
h_g = vertical distance measured from the ground plane
J = payoff function
m = mass of the helicopter
P_d = power difference in steady level flight
R = radius of rotor
R/C = rate of climb
S_r = reference distance
T = thrust
t = time
v_{i0} = induced velocity
V = velocity of the helicopter
V_m = smallest velocity where equilibrium flight of the helicopter out of ground effect is possible
V_r = reference velocity: induced velocity at hover out of ground effect
V_{s1} = static best climb angle speed
V_{s2} = static best rate of climb speed
W = weight
x_g = horizontal distance measured on the ground plane
Z = vertical height of the rotor above the ground plane
α_{TP} = angle of attack of the rotor tip path plane
β = $d\gamma/dt$ = control variable
η = dV/dt = control variable
γ = flight path angle
δv_{i0} = effective reduction of induced velocity of the rotor due to ground effect
λ_H = inflow through the rotor plane nondimensionalized by ΩR
π = 3.1416
ρ = density of air
τ = nondimensional time
Ω = rotational frequency of the helicopter rotor
$\bar{\ }$ = nondimensional quantity
∂ = partial derivative
d = total derivative
( ) = is a function of

Subscripts

f = final
g = ground axis system; inclusion of ground effect in vehicle performance equations
i = initial
r = reference trajectory

Presented as Paper 70-931 at the AIAA 2nd Aircraft Design and Operations Meeting, Los Angeles, Calif., July 20–22, 1970; submitted August 3, 1970; revision received May 6, 1971.
Index Category: VTOL Flight Operations.
* Research Scientist, U.S. Army Air Mobility Research & Development Laboratory—Ames Directorate. Associate Member AIAA.

Introduction

THE increasing mobility requirements of the United States Army in the 1960's created a place for the helicopter as a close support aircraft. Its hovering capability has allowed the helicopter to be used as a "flying truck" by lifting men and supplies to and from unprepared landing sites. In many cases, the helicopter is the only available means of evacuating injured or surrounded troops from a hostile area. In these difficult and frequently occurring situations, obtaining maximum pilot-vehicle performance during takeoff may be the difference between mission failure or success.

By design, the helicopter is capable of lifting, out-of-ground effect, its normal operating payload under standard atmospheric conditions. This vertical takeoff capability is very seldom used as a piloting technique because of safety considerations. It is sensible to accelerate to some forward speed before climbing, in case of engine failure. If the engine does fail in a single-engine helicopter at forward speed, some of the kinetic energy of translation may be used to perform the landing flare associated with autorotative flight.

In many operational situations, geographical factors and mission requirements force the helicopter to operate far from its design conditions. Hot days, high altitudes, and heavy payloads often degrade the performance of the helicopter to the point where hovering out-of-ground effect is not possible. In these heavily loaded (HLD) conditions, hovering flight in ground effect may still be feasible. However, very little excess power is available to accelerate the helicopter to sufficient translational velocity where climbing flight out-of-ground effect can be maintained. Under these operating conditions, the HLD helicopter must perform a STOL takeoff.

If the horizontal takeoff distance of this HLD helicopter is constrained by the operating environment (Fig. 1), it may be necessary to obtain the optimum pilot-vehicle performance during takeoff. This type of operational situation is frequently encountered in Vietnam. A rescue helicopter is dispatched to a remote landing area to evacuate troops in a hostile area. The tropical climate and operating altitude limit the rescue helicopter's performance. During the rescue operation, the payload of the helicopter is increased and the helicopter often becomes heavily loaded. Taking off under these conditions in a confined area quickly became the mark of a "good pilot." In fact, it is understood among veteran pilots that some pilots are better than others at performing this tricky and difficult maneuver.

In this paper, the maximum performance takeoff of a heavily loaded helicopter is investigated. The objective of the analysis was to understand the important performance parameters of the problem and to devise a simplified near-optimal takeoff technique which could be instrumented to improve the pilot-vehicle performance. It was understood at the outset that some pilots were very proficient at this takeoff task and that they would probably derive very little

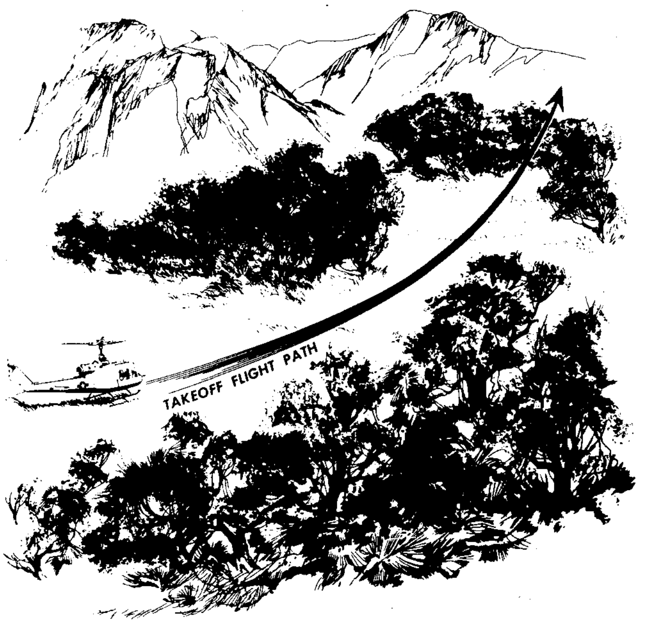

Fig. 1 Aerial view of the operational environment often encountered under heavily loaded conditions.

from this effort. However, most of the helicopter pilots who were consulted did consider some type of instrumentation or display aid desirable and helpful. Any simple instrumentation to measure and improve takeoff performance under these severe circumstances was welcomed.

The theoretical maximum performance HLD helicopter takeoff problem is illustrated in Fig. 2. Simply stated, the objective of the theoretical analysis is to determine the extremal trajectory of an HLD helicopter which maximizes the terminal vertical distance (h_g) for a given fixed horizontal takeoff distance (x_g). By optimizing the vertical height at the terminal horizontal distance, the safety margin shown in Fig. 2 is maximized, thus reducing the risk of colliding with the obstacle.

Optimal control theory is a tool which has been used to theoretically investigate this dynamic maneuver. Emphasis has been placed upon understanding the performance tradeoffs associated with constrained and unconstrained mathematically optimal solutions. Many of the theoretical details of the interaction of optimal control theory with the dynamic model building process have been omitted from this paper. The interested reader is asked to consult Ref. 1 for a more rigorous presentation of the mathematics.

Performance Equations

The dynamic performance of a HLD helicopter operating in ground effect can be described mathematically by the simple power balance equation given below. A complete derivation of this equation is

$$\underbrace{\bar{P}_{dav}}_{\substack{\text{Power}\\\text{difference}\\\text{available}}} - \underbrace{\bar{v}_{i0}}_{\substack{\text{Induced}\\\text{power}}} + \underbrace{\delta\bar{v}_{i0}}_{\substack{\text{Ground}\\\text{effect}\\\text{power}}} - \frac{\partial\lambda_H}{\partial\alpha_{TP}}\bigg|_r \Big[\underbrace{\gamma}_{\substack{\text{Climb}\\\text{power}}} + \underbrace{\frac{f}{4A}\bar{V}^2}_{\substack{\text{Parasite}\\\text{drag}\\\text{power}}}\Big] =$$

$$\underbrace{\frac{\partial\lambda_H'}{\partial\alpha_{TP}}\bigg|_r \frac{d\bar{V}}{d\tau}}_{\substack{\text{Tangential}\\\text{acceleration}\\\text{power}}} + \underbrace{[C_1 + \bar{v}_{i0} - \delta\bar{v}_{i0}]V\frac{d\gamma}{d\tau} + C_5\left[\bar{V}\frac{d\gamma}{d\tau}\right]^2}_{\text{Curvature power}} \quad (1)$$

presented in Ref. 1. It has been assumed in this problem that the HLD helicopter does not make contact with the ground plane. It may be argued that helicopter performance may be increased by allowing a ground contact segment. However, maintaining ground contact in rough terrain is difficult and dangerous with heavy payloads. For this reason, this type of maximum performance takeoff has not been allowed (Ref. 2).

Equation (1) describes the dynamic tradeoffs which are possible. It should be noted that this equation is singular at $\bar{V} = 0$. This problem arises because the basic wind axis system is ill-defined. However, at near zero forward speeds, a constant acceleration segment is a good approximation to helicopter performance. Therefore, it has been assumed that all HLD helicopter takeoffs are initiated with a constant acceleration segment. When $\bar{V} \geq 0.5$, the given performance equation is valid.

The first term in Eq. (1) is the power difference available ($\bar{P}_{dav}$). It is composed of two parts, a power input term and a power loss term. During a maximum performance takeoff, all available shaft horsepower is delivered to the helicopter rotor system. Assuming that the rotor rpm does not vary, this maximum power input term is represented by the constant P_{av}. The sum of rotor profile power, tail anti-torque power, and engine installation power losses is represented by the power loss term CPL. For simplicity, it has been assumed that the variations of CPL with forward velocity and inflow angle of the tip-path-plane can be neglected. The net power difference available term (P_{dav}) is now defined as the difference between the P_{av} and the CPL. This quantity is nondimensionalized by the induced power in hover yielding

$$\bar{P}_{dav} \equiv (P_{av} - CPL)/WV_r \quad (2)$$

The amount of power necessary to maintain a rotor in equilibrium flight at various forward velocities is theoretically obtained by applying simple momentum theory to the rotor tip path plane. Assuming also that the disk itself is at zero angle of attack to the velocity vector of the vehicle, an explicit expression for nondimensionalized induced power ($\bar{v}_{i0}$) is obtained:

$$\bar{v}_{i0} = [-(\bar{V}^2/2) + (\bar{V}^4/4 + 1)^{1/2}]^{1/2} \quad (3)$$

Physically, this term is analogous to an airplane's induced power loss.

The parasite drag of a helicopter can be represented by an equivalent flat plate drag area times the dynamic pressure. The nondimensionalized power required to drag this flat plate through the air at a given velocity is given by the term

$$+\ \partial\lambda_H'/\partial\alpha_{TP}|_r\bar{V}^2(f/4A)$$

In Fig. 3, the parasite drag, induced and $\bar{P}_{dav}$ power terms are presented in nondimensionalized form for the single rotor helicopter chosen in Appendix A.

A rotor operating near the ground plane experiences an effective rise in the power available in hover and at slow forward speeds. This effective rise in the power available results when the downwash impinges upon the ground plane, creating an "air-cushion effect." Pilots speak of leaving the influence of ground effect as forward flight is attained as "flying off the bubble." The term $\delta\bar{v}_{i0}$, which is plotted in Fig. 4, represents this effective increase in power available with height above the ground and forward velocity of the vehicle as the major parameters. It is discussed in detail in Refs. 3 and 4.

The total power available in level steady-state flight is obtained by adding all of the power source terms and subtracting all of the power loss terms. The expression for this power

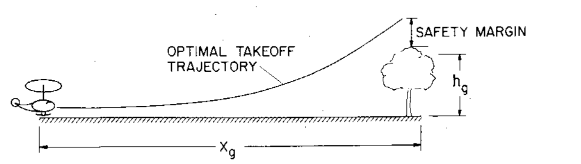

Fig. 2 An illustration of the optimal takeoff trajectory of an HLD helicopter.

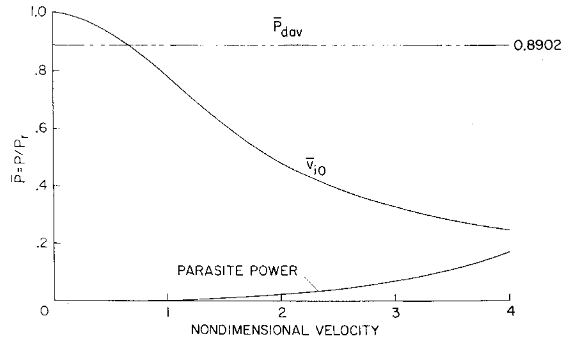

Fig. 3 Basic helicopter power terms vs velocity.

difference becomes

$$\bar{P}_{dg}(\bar{V}, \bar{h}_g) = [P_{dav} - \bar{v}_{i0} + \delta\bar{v}_{i0}] - \partial\lambda_H'/\partial\alpha_{TP}|_r \bar{V}^2(f/4A) \quad (4)$$

In Fig. 5, this power difference expression is plotted at three different rotor heights above the ground. At small Z/R, some excess power is available to begin the maximum performance takeoff.

The remaining term on the left side of the basic power balance equation [Eq. (1)] represents the amount of additional power that is necessary to maintain steady-state climbing flight out-of-ground effect. It is mathematically expressed as

$$\partial\lambda_H'/\partial\alpha_{TP}|_r\gamma$$

The terms on the right-hand side of Eq. (1) determine the amount of power that is required to perform dynamic maneuvers. The first term,

$$\partial\lambda_H'/\partial\alpha_{TP}|_r d\bar{V}/d\tau$$

is a measure of the power increment necessary to accelerate the helicopter tangentially along the flight path. The remaining two terms on the right-hand side of Eq. (1) measure the amount of power required to curve the flight path.†

The factor

$$\partial\lambda_H'/\partial\alpha_{TP}|_r$$

which appears with the parasite drag, climb, and tangential acceleration terms in Eq. (1), is a measure of the increase in inflow through the rotor due to changes in the rotor tip-path-plane angle of attack. The angle of attack change is required to achieve a longitudinal force balance equilibrium. The net effect is to reduce the power required in some low-speed maneuvers.

For convenience in interpretation, Eq. (1) may be multiplied by the quantity

$$\bar{V}/(\partial\lambda_H'/\partial\alpha_{TP})|_r$$

A new power difference expression ($\bar{P}_{dg}'$) which implicitly includes the tip-path-plane angle-of-attack effects is defined as

$$\bar{P}_{dg}'(\bar{V},\bar{h}_g) \equiv [\bar{V}/(\partial\lambda_H'/\partial\alpha_{TP})|_r]\bar{P}_{dg}(\bar{V},\bar{h}_g) \quad (5)$$

This expression is plotted in Fig. 6 as a function of rotor height above the ground plane and forward velocity. This new definition allows the dynamic optimization problem to be approached from the classical static helicopter performance problem. Using this definition and the preceding manipulations, Eq. (1) becomes

$$\frac{\bar{P}_{dg}'(\bar{V},\bar{h}_g)}{\bar{V}} - \gamma = \frac{d\bar{V}}{d\tau} + \left\{[C_1 + \bar{v}_{i0} - \delta\bar{v}_{i0}]\bar{V}\left(\frac{d\gamma}{d\tau}\right) + C_5\left[\bar{V}\frac{d\gamma}{d\tau}\right]^2\right\} \Bigg/ \frac{\partial\lambda_H'}{\partial\alpha_{TP}}\Bigg|_r \quad (6)$$

† It is desirable to retain the flight path curvature terms to second-order in the power balance equation to avoid singular optimization problems. This topic is discussed at length in Ref. 1.

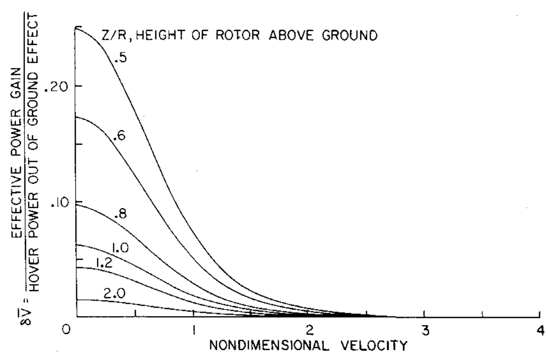

Fig. 4 Effective increase in helicopter power due to ground proximity vs velocity.

Static helicopter performance out-of-ground effect occurs when $d\bar{V}/d\tau \equiv d\gamma/d\tau \equiv 0$, and $\bar{h}_g$ becomes large.

Equation (6) then becomes

$$\bar{P}_d'(\bar{V}) = V\gamma \quad (7)$$

A plot of $\bar{P}_{dg}'(\bar{V},h_g \to \text{large}) \equiv P_d'(V)$ is presented in Fig. 7. The velocity at which the best steady-state out-of-ground effect rate of climb is achieved ($\bar{V}_{s2}$) is located by finding the point where the power difference function $[P_d'(V)]$ reaches a maximum. The best rate of climb is then given by Eq. (7).

To determine the velocity where the best steady-state climb angle is achieved, a straight line through the origin of the plot of $\bar{P}_d'$ vs $\bar{V}$ is constructed such that it becomes tangent to the $\bar{P}_d'$ curve. The point of tangency locates the velocity at which the maximum steady-state climb angle is achieved ($\bar{V}_{s1}$). The resulting climb angle is found from Eq. (7).

Optimal Takeoff Problem Formulation (Unconstrained)

An illustration of the maximum dynamic performance problem which is considered in this paper is presented in Fig. 2. The objective of the analysis is to determine the extremal trajectory that maximizes the terminal vertical distance (h_g) for a given fixed horizontal takeoff distance (x_g). Assuming that the flight path angles considered are small, this problem is mathematically formulated in modern control theory notation as follows:

Maximize

$$J \equiv \int_i^f \frac{d\bar{h}_g}{d\tau}\, d\tau = \int_i^f \bar{V}\gamma d\tau \quad (8)$$

subject to the mathematical performance equations

$$d\bar{V}/d\tau = \bar{P}_{dg}'(\bar{V},\bar{h}_g)/\bar{V} - \gamma - \{[C_1 + \bar{v}_{i0} - \delta\bar{v}_{i0}] \times \bar{V}(V_r/g)\beta + C_5[\bar{V}(V_r/g)\beta]^2\} \Bigg/ \frac{\partial\lambda_H'}{\partial\alpha_{TP}}\Bigg|_r \quad (9)$$

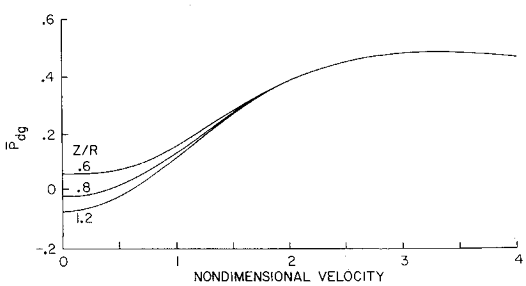

Fig. 5 Power difference curves of a helicopter operating in ground effect at constant altitudes vs velocity without rotor plane linear angle of attack effects.

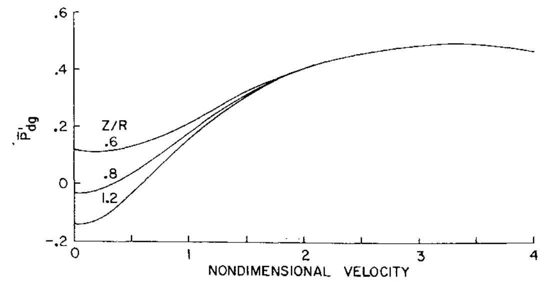

Fig. 6 Power difference curves of a helicopter operating in ground effect.

$$d\gamma/d\tau = (V_r/g)\beta \tag{10}$$

$$d\bar{x}_g/d\tau = \bar{V} \tag{11}$$

The mathematical control of this system of equations is chosen to be β, the rate of change of the flight path angle with respect to real time. The change in the flight path angle with respect to nondimensional time τ is given by Eq. (10). The last performance equation given relates the tangential velocity of the helicopter to the horizontal distance in the chosen ground-based axis system.

Because these performance equations are singular at $\bar{V} = 0$, a constant 0.2 g acceleration segment at constant skid height above the ground plane has been assumed until $\bar{V} = 0.5$. This first takeoff segment (H/1) has a distance parallel to the ground of $\bar{x}_{g1} = 1.25$ ($x_{g1} = 60.4$ ft).

Furthermore, the HLD helicopter considered in this analysis cannot maintain steady-state flight out-of-ground effect until $\bar{V}_m = 0.7$. Therefore, it is unnecessary to start an optimization problem until this velocity is attained. If all of the available power is used to accelerate the aircraft to this critical velocity from the end of the first segment, an additional distance parallel to the ground of $\bar{x}_{g2} = 0.48$ ($x_{g2} = 23.2$ ft) is accumulated.

The total distance parallel to the ground plane, which is flown by the helicopter before the maximum performance trajectory may be initiated, is the sum of these two restricted segments. For the helicopter considered in this analysis, $\bar{x}_{g1} + \bar{x}_{g2} = 1.73$ ($x_{g1} + x_{g2} = 83.6$ ft).

The interesting optimization problem really begins at the initial conditions $\bar{V}_i = 0.7$, $\gamma_i = 0$, $\bar{x}_{gi} = 1.73$, and $\bar{h}_{gi} = 0.04$ ($h_g \approx 2$ ft). This last segment of the problem where dynamic performance tradeoffs are possible is called segment H-3. The terminal conditions are chosen to be $\bar{V}_f = 0.7$, $\gamma_f =$ free, and $\bar{x}_{gf} = 11.73$.

Near the terminal horizontal distance, additional altitude can be gained by allowing the helicopter to trade kinetic for potential energy. By specifying the terminal condition on velocity to be the smallest velocity for level equilibrium flight out-of-ground effect, the helicopter is prevented from entering unsafe regions of state space.

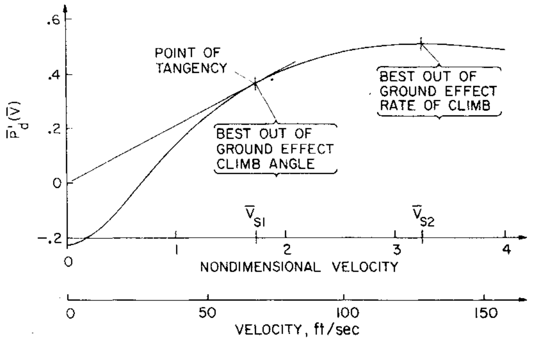

Fig. 7 Power difference curve of an HLD helicopter operating out-of-ground effect vs velocity.

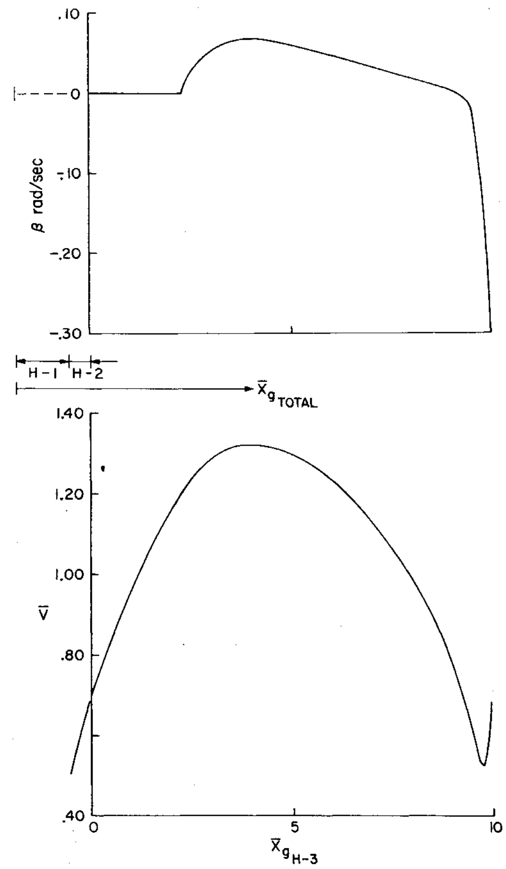

Fig. 8 HLD helicopter; flight path rate and velocity vs horizontal distance.

If the Hamiltonian of the problem formulation is developed[1] and the necessary conditions for a local extremum are applied, a nonlinear two-point boundary value problem results. The inclusion of the second-order term in the power equation due to flight path curvature has insured that the resulting boundary value problem is nonsingular. However, because the change in power due to a change in thrust has only been retained to first order, the performance equation can rigorously be considered to be valid to first order only. The reason for retaining the second-order term is that the unconstrained singular boundary value problem which would arise if the flight path curvature had been retained to first order was numerically unsolvable at this time.[1]

Solution Using a Modified Gradient Projection Algorithm

To solve the atmospheric trajectory optimization problem presented, a nonsingular two-point boundary value problem must be solved. The technique that was used with considerable success was a modified gradient projection algorithm. Appendix XIII in Ref. 1 discusses some of the useful modifications that were added to the gradient projection programs presented in Refs. 5–7 which were necessary to arrive at the solutions presented.

At first, the digital computer solutions for the HLD helicopter supported solely by aerodynamic forces passed through the ground plane. This initial dive increased the acceleration capability of the helicopter permitting unrealistic but mathematically optimal trajectories to be determined. A state space altitude inequality constraint was enforced limiting the helicopter to operation at or above its initial hovering height ($\bar{h}_{gi} = 0.04$).

The numerical procedure used to enforce the constraint was suggested in Ref. 8. The maximum performance seg-

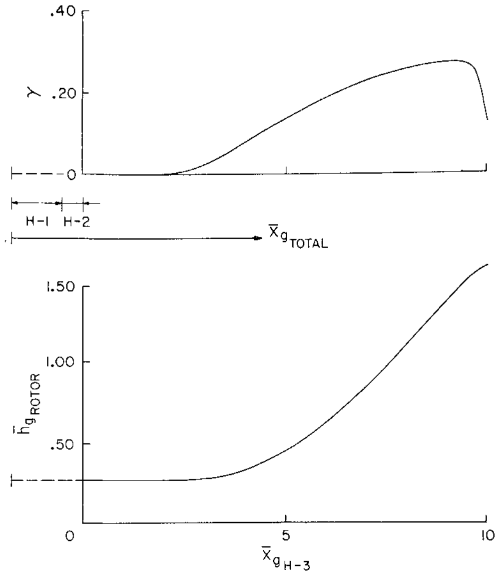

Fig. 9 HLD helicopter; flight-path angle and vertical distance vs horizontal distance.

ment was further segmented into two subphases, a constrained and unconstrained segment. Both subphases were joined to meet the system boundary conditions resulting from the enforcement of the altitude state space inequality constraint. The procedure is discussed in detail in Ref. 1.

The extremal control and resulting trajectory for the maximum performance segment of the HLD helicopter are shown in Figs. 8 and 9. The helicopter accelerates initially at constant height above the ground plane to achieve higher values of level steady-state power difference $\{P_{d_g}'\}$ and to accumulate translational kinetic energy. Slightly before half of the total phase H-3 distance is attained, the helicopter begins to decelerate. This deceleration maneuver is maintained throughout most of the remaining phase H-3 distance. Most of the altitude that is gained by the helicopter is attained during this deceleration when kinetic energy is being exchanged for potential energy. To satisfy the specified terminal condition on velocity, a negatively curving trajectory is performed near the final time. The additional excess power resulting from this maneuver enables the helicopter to accelerate to the specified terminal velocity.

In the problems treated in this paper, the horizontal distances considered did not allow a maximum steady-state climbing segment to appear. However, as the specified horizontal distance is increased, such a segment is asymptotically approached. In Ref. 1, a simplified modeling technique is presented which highlights this observation.

By obtaining a number of extremal dynamic trajectories at chosen values of fixed horizontal distance, a plot of optimum altitudes ($\bar{h}_{g_f}^*$) vs the chosen horizontal distance ($\bar{x}_{g\text{TOTAL}}$) can be obtained (see Fig. 10).

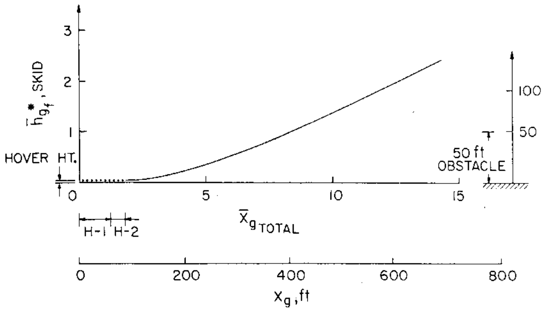

Fig. 10 Locus of extremal trajectories of the skid height of an HLD helicopter constrained to fly above the ground plane vs horizontal distance.

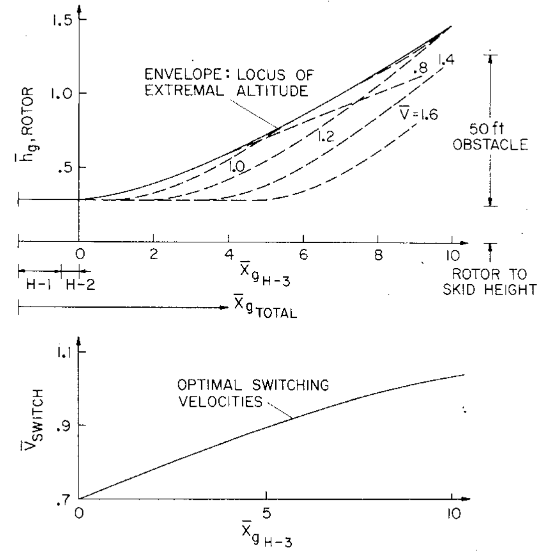

Fig. 11 Locus of extremal altitudes and optimal switching velocities vs nondimensional horizontal distance.

The takeoff distance needed to clear an obstacle of a fixed height can easily be read off this graph. To clear a 50-ft obstacle with a safety margin of zero, a total takeoff distance of 410 ft is needed ($\bar{x}_{g\text{TOTAL}} = 8.49$) for the helicopter model given in Appendix A.

Optimal Takeoff Trajectories with a Nondecelerating Constraint

Although the final unconstrained extremal trajectory of the dynamic helicopter model is physically realizable, it would take a very proficient pilot to fly the resulting trajectory. If too much kinetic energy is traded for potential energy too soon during the deceleration portion of the trajectory, the pilot would find himself in danger. His reduced speed would preclude his obtaining maximum performance. Because the net power excess is very sensitive to small changes in velocity at low forward speeds, maintaining horizontal flight below $\bar{V}_m$ is impossible. His only recourse would be to decelerate to zero velocity (if there was enough horizontal distance left), come to hover near the terminal point, and try again.

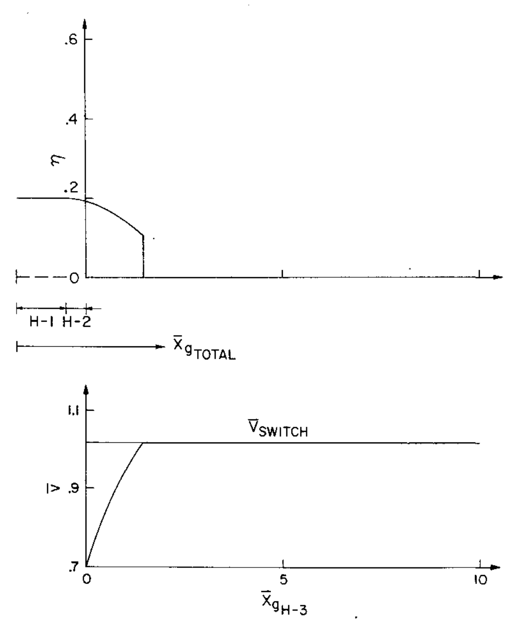

Fig. 12 Optimal acceleration and velocity histories vs nondimensional horizontal distance.

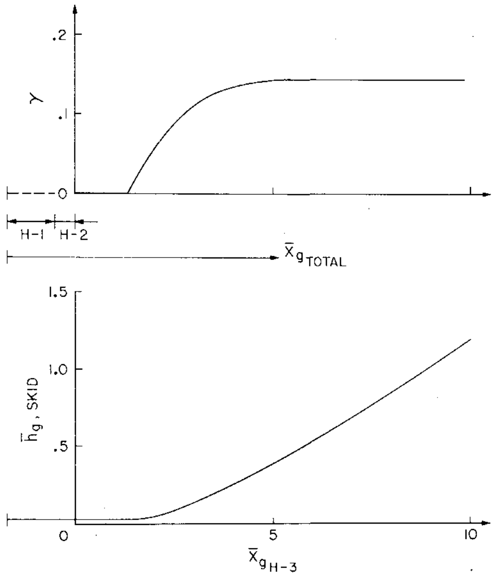

Fig. 13 Optimal flight path angle and altitude histories vs nondimensional horizontal distance.

A class of problems which would be much easier to fly would consist of only optimal nondecelerating trajectories. Because the class of solutions has been restricted a priori, some takeoff performance must be sacrificed. However, because these restricted trajectories are easier to fly, they may be operationally more useful. Less experienced pilots should be able to fly the constrained optimal trajectories with very little practice.

A slightly different formulation of the takeoff optimization problem is needed to allow the nondecelerating constraint to be easily enforced. The mathematical control of this new problem formulation is chosen to be

$$dV/dt \equiv \eta \text{ (acceleration control)}$$

Therefore, nondecelerating trajectories are bounded from below by the control constraint that

$$\eta \geq 0 \tag{12}$$

To simplify the mathematics, the second-order flight path curvature in the performance equation [Eq. (6)] is neglected. The resulting performance equation becomes

$$\frac{\bar P_{d_g}'(\bar V,\bar h_g)}{\bar V} - \gamma = \frac{d\bar V}{d\tau} + \left\{[C_1 + \bar v_{i0} - \delta\bar v_{i0}]\bar V \Big/ \frac{\partial\lambda_H'}{\partial\alpha_{TP}}\Big|_r\right\}\frac{d\gamma}{d\tau} \tag{13}$$

If the following definition is introduced

$$[C_1 + \bar v_{i0} + \delta\bar v_{i0}]\bar V/(\partial\lambda_H'/\partial\alpha_{TP})|_r \equiv D(\bar V,\bar h_g) \tag{14}$$

the resulting performance equation becomes

$$\bar P_{d_g}'(\bar V,\bar h_g)/\bar V - \gamma = (d\bar V/d\tau) + D(\bar V,\bar h_g)(d\gamma/d\tau) \tag{15}$$

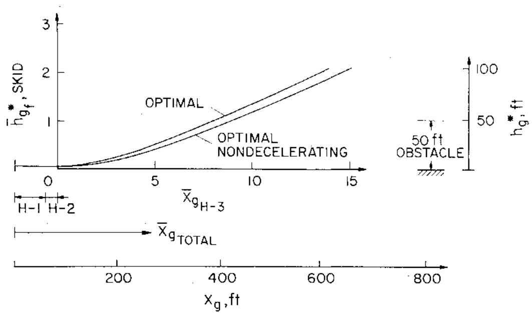

Fig. 14 Locus of extremal heights vs horizontal distances.

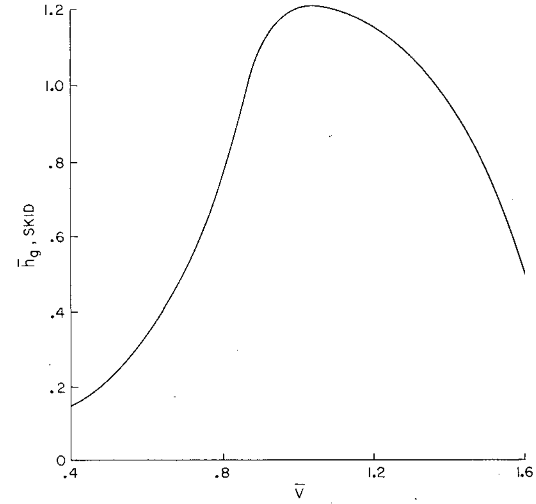

Fig. 15 Obtainable height as a function of velocity for a given takeoff distance.

This equation, like Eq. (6), describes dynamic helicopter performance to first order (see Ref. 1).

The modern control theory formulation of the constrained takeoff problem becomes:
Maximize

$$J \equiv \int_i^f \frac{d\bar h_g}{d\tau}\, d\tau = \int_i^f \bar V \gamma d\tau \tag{8}$$

subject to the mathematical performance equations

$$d\bar V/d\tau = (V_r/g)\eta \tag{16}$$

$$d\gamma/d\tau = 1/[D(\bar V,\bar h_g)]\{P_{d_g}'(\bar V,\bar h_g)/\bar V - \gamma - (V_r/g)\eta\} \tag{17}$$

$$d\bar x_g/d\tau = \bar V \tag{11}$$

The initial conditions of this new problem formulation are identical to the preceding case. However, the terminal condition on velocity does not have to be enforced. The nondecelerating constraint insures that the helicopter is always operating in safe regions of state space. The initial and terminal conditions become:
initial conditions

$$\bar V_i = 0.7,\ \gamma_i = 0,\ \bar x_{gi} = 1.73,\ \bar h_{gi} = 0.04\ (h_g \approx 2 \text{ ft})$$

terminal conditions

$$\bar V_f = \text{free},\ \gamma_f = \text{free},\ \bar x_{gf} = 11.73$$

The necessary conditions for a local extremum of this restricted problem formulation are presented in Ref. 9. Because the mathematical control η appears linearly, the optimal control is of a "bang-bang" nature. However, the possibility of having singular arcs appear in the resulting two-point boundary value problem also exists. This possibility is explored in Ref. 9 where it is shown that along the singular candidate segments, the helicopter control becomes

$$\eta \leq 0 \tag{18}$$

However, the maximum principle has allowed as candidates for the solution only those trajectories that obey Eq. (12). The conclusion is that only the singular solution $\eta = 0$ is a possible candidate segment. However, this singular control is identical to the lower control bound already specified. This result simplifies the solution of the resulting two-point boundary value problem tremendously. The singular solution candidates are now identical to the lower control limited candidates. The optimal control consists of a pure bang-bang control [$\eta = \eta_{\max}$ or $\eta = 0$].

The upper control bound is governed by the implicit constraint that diving flight is prohibited in the analysis. Thus, if $\gamma = 0$, $d\gamma/d\tau$ must equal zero. The resulting upper bound becomes

$$\eta_{\max} = (g/V_r)P_{dg}'(\bar{V},\bar{h}_g)/\bar{V} \quad (19)$$

when $\gamma = 0$.

In all of the problems treated in this paper, the mathematical control has exhibited only one switch [from $\eta = \eta_{\max}$ to $\eta = 0$]. Therefore, a simple graphical procedure suggested in Ref. 8 can be used to find the constrained optimal trajectory that meets the given boundary conditions of the problem. This procedure is illustrated in Fig. 11 for the helicopter described in Appendix A.

In essence, the boundary value problem is flooded with all possible combinations of allowed control time histories. Specifically, the maximum acceleration segment [Eq. (19)] is integrated until a chosen switching velocity ($\bar{V}_{\text{switch}}$) is attained. At this point, the control η is set equal to zero, the remaining part of the trajectory is calculated, and the results are drawn upon the $\bar{h}_g$ vs $\bar{x}_g$ plot shown (Fig. 11). The process is repeated a number of times with switching velocities that are less than the velocity at which the best out-of-ground effect climb is achieved. The envelope of the resulting curves then becomes the locus of the optimal altitudes for any given horizontal distance. The optimal switching velocities for the locus of optimal trajectories is also illustrated in Fig. 11.

For a horizontal distance of $\bar{x}_{g\text{TOTAL}} = 11.73$, the optimal control and resulting trajectory are illustrated in Figs. 12 and 13. At first, the helicopter accelerates at constant height to gain velocity. As its velocity increases, larger values of excess power become available. The second segment of the optimal trajectory begins when the helicopter attains the optimal switching velocity that corresponds to a total horizontal distance of $\bar{x}_g = 11.73$. The vehicle then maintains a constant velocity using all of its excess power available to rotate and climb over the obstacle.

The optimal nondecelerating trajectory, as illustrated in Figs. 12 and 13, is relatively simple to fly. However, some takeoff performance has been sacrificed for increased simplicity. Just how much can be seen in Fig. 14, where the locus of extremal altitudes ($\bar{h}_{gf}^*$) vs horizontal distance ($\bar{x}_{g\text{TOTAL}}$) for the unconstrained and constrained trajectories is illustrated. For obstacles of about 50 ft in height, the optimal nondecelerating trajectories require about a 10% increase in field takeoff length.

Another important consideration to bear in mind when evaluating takeoff performance, is the sensitivity of the optimal performance to nonoptimal deviations in control. Such a situation may exist if the pilot attains his constant velocity climbout segment too early or too late. His nonoptimal performance is plotted vs switching velocity for one field length ($\bar{x}_g = 11.73$) in Fig. 15. It can be seen from this figure that at constant velocity climbouts at velocities less than the optimal climbout velocity, performance deteriorates rapidly. At velocities higher than the optimal, performance also deteriorates. However, in an operational situation, the pilot has the option of trading some of this excess velocity for potential energy at will. The net effect is to reduce the sensitivity of the optimal nondecelerating solutions to higher than optimum switching velocity variations.

Conclusions

The major results of this paper may be highlighted by comparing the advantages and disadvantages of both of the takeoff techniques presented.

The unconstrained optimal takeoff technique begins with a maximum acceleration segment where the helicopter flies parallel to, but off the ground plane. Close proximity to the ground plane is maintained to take advantage of the apparent power gain due to ground effect. This maximum acceleration segment is followed by a climbing and accelerating segment followed in turn by a climb and deceleration segment. In the last phase of the takeoff maneuver, the helicopter accelerates and decreases its rate of climb to meet the terminal condition on velocity. Most of the altitude gained during this dynamic maneuver is gained during the deceleration segment.

The major advantage of the optimal unconstrained takeoff technique is that best system performance is achieved. For a given horizontal distance, maximum vertical height is attained. Or, for a given obstacle height, the shortest takeoff distance is required. The major disadvantage of the technique is that an extreme degree of piloting skill is required to fly the optimal trajectory. Perhaps a flight director which combines an accurate measurement of vehicle velocity and excess power in a dynamic situation display would be of use to the pilot. If this type of situation display were available, significant increases in takeoff performance could be expected by use of the optimal takeoff technique.

The major advantage of the optimal nondecelerating trajectories is their simplicity. The optimal control policy is basically independent of the problem's boundary conditions. It consists of a bang-bang control with only one switch. Furthermore, all accelerating flight is done horizontally near the ground plane up to a relatively safe speed in case of engine failure. The helicopter then performs a constant velocity climbout until the obstacle is cleared. The major disadvantage of this takeoff technique is that some takeoff performance is sacrificed to enforce the nondeceleration constraint.

Appendix A: Performance Characteristics of the HLD Helicopter

The performance characteristics of the HLD helicopter used in this paper are presented below. The model closely resembles the UH1-B helicopter

$$A = 1400 \text{ ft}; \qquad W = 9000 \text{ lb}$$

$$\rho = 2.07 \cdot 10^{-3} \text{ slug/ft}^3 (\text{at } 2000 \text{ ft}, 90°\text{F})$$

$$P_{av} = 820 \text{ hp (at 2000 ft, 90°F)}$$

$$f = 15 \text{ ft}^2; \qquad f/4A = 0.002678$$

$$CPL = 30\%\ P_{av} = 246 \text{ hp}$$

$$V_r = (W/2\rho A)^{1/2} = 39.4 \text{ fps}$$

$$S_r = V_r^2/g = 48.3 \text{ ft}; \qquad \bar{P}_{dav} = 0.8902; \qquad P_r = 644.7 \text{ hp}$$

References

[1] Schmitz, F. H., "Takeoff Optimization for STOL Aircraft and Heavily Loaded Helicopters," TR-ECOM-02412-4, Aug. 1969, U.S. Army Electronics Command, Fort Monmouth, N. J.

[2] Mills, J. W. and Durbin, E. J., "Aerodynamic Instrumentation for Improving Helicopter Takeoff and Landing Piloting Performance," *Proceedings of the Fifth International Aerospace Instrumentation Symposium*, Cranfield, March 25–28, 1968.

[3] Katzoff, S. and Sweberg, H. H., "Ground Effect on Downwash Angles and Wake Location," Rept. 738, 1942, NACA.

[4] Cheesman, I. C. and Bennett, W. E., "The Effect of the Ground on a Rotor in Forward Flight," Reports and Memoranda 3021, Sept. 1955, Aeronautical Research Council, Great Britain.

[5] Rozen, J. B., "The Gradient Projection Method for Nonlinear Programming," Pts. 1 and 2, *Journal of the Society for Industrial and Applied Mathematics*, Vol. VIII, No. 1, March 1960, pp. 181–218.

[6] Bryson, A. E., Jr. and Denham, W. T., "A Steepest-Ascent Method for Solving Optimum Programming Problems," *Journal of Applied Mechanics*, June 1962, pp. 247–257.

[7] Stein, L. H., Matthews, M. L., and Frank, J. W., "STOP—A Computer Program for Supersonic Transport Optimization," CR-793, May 1967, NASA.

[8] Schmitz, F. H., "Takeoff Trajectory Optimization of a Theoretical Model of a STOL Aircraft," AIAA Paper 69-935, Princeton, N. J., 1969.

[9] Schmitz, F. H. and Born, G., "A Sensitivity Analysis of Constrained Optimal Heavily Loaded Helicopter Takeoff Performance," Report, ECO, U.S. Army Electronics Command, to be published.